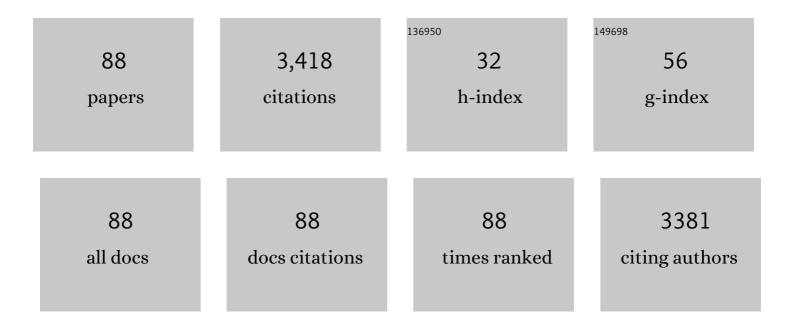
Qingyi Zeng

List of Publications by Year in descending order

Source: https://exaly.com/author-pdf/3013857/publications.pdf Version: 2024-02-01



#	Article	IF	CITATIONS
1	Electronic Structure Modulation of Graphitic Carbon Nitride by Oxygen Doping for Enhanced Catalytic Degradation of Organic Pollutants through Peroxymonosulfate Activation. Environmental Science & Technology, 2018, 52, 14371-14380.	10.0	455
2	A highly efficient BiVO 4 /WO 3 /W heterojunction photoanode for visible-light responsive dual photoelectrode photocatalytic fuel cell. Applied Catalysis B: Environmental, 2016, 183, 224-230.	20.2	151
3	Synthesis of WO3/BiVO4 photoanode using a reaction of bismuth nitrate with peroxovanadate on WO3 film for efficient photoelectrocatalytic water splitting and organic pollutant degradation. Applied Catalysis B: Environmental, 2017, 217, 21-29.	20.2	134
4	High-performance BiVO4 photoanodes cocatalyzed with an ultrathin α-Fe2O3 layer for photoelectrochemical application. Applied Catalysis B: Environmental, 2017, 204, 127-133.	20.2	133
5	Highly selective transformation of ammonia nitrogen to N2 based on a novel solar-driven photoelectrocatalytic-chlorine radical reactions system. Water Research, 2017, 125, 512-519.	11.3	127
6	Preparation of vertically aligned WO3 nanoplate array films based on peroxotungstate reduction reaction and their excellent photoelectrocatalytic performance. Applied Catalysis B: Environmental, 2017, 202, 388-396.	20.2	114
7	Highly nitrogen-doped porous carbon transformed from graphitic carbon nitride for efficient metal-free catalysis. Journal of Hazardous Materials, 2020, 393, 121280.	12.4	105
8	A solar light driven dual photoelectrode photocatalytic fuel cell (PFC) for simultaneous wastewater treatment and electricity generation. Journal of Hazardous Materials, 2016, 311, 51-62.	12.4	103
9	Biomimicry of bamboo bast fiber with engineering composite materials. Materials Science and Engineering C, 1995, 3, 125-130.	7.3	98
10	Highly-stable and efficient photocatalytic fuel cell based on an epitaxial TiO2/WO3/W nanothorn photoanode and enhanced radical reactions for simultaneous electricity production and wastewater treatment. Applied Energy, 2018, 220, 127-137.	10.1	87
11	Enhanced organic pollutants degradation and electricity production simultaneously via strengthening the radicals reaction in a novel Fenton-photocatalytic fuel cell system. Water Research, 2017, 108, 293-300.	11.3	84
12	Construction of g-C3N4/WO3/MoS2 ternary nanocomposite with enhanced charge separation and collection for efficient wastewater treatment under visible light. Chemosphere, 2020, 247, 125784.	8.2	80
13	A novel in situ preparation method for nanostructured α-Fe ₂ O ₃ films from electrodeposited Fe films for efficient photoelectrocatalytic water splitting and the degradation of organic pollutants. Journal of Materials Chemistry A, 2015, 3, 4345-4353.	10.3	79
14	Efficient inhibition of photogenerated electron-hole recombination through persulfate activation and dual-pathway degradation of micropollutants over iron molybdate. Applied Catalysis B: Environmental, 2019, 257, 117904.	20.2	79
15	Highly-active, metal-free, carbon-based ORR cathode for efficient organics removal and electricity generation in a PFC system. Chinese Chemical Letters, 2021, 32, 2212-2216.	9.0	70
16	BiVO4/TiO2(N2) Nanotubes Heterojunction Photoanode for Highly Efficient Photoelectrocatalytic Applications. Nano-Micro Letters, 2017, 9, 14.	27.0	66
17	Insights into the difference in metal-free activation of peroxymonosulfate and peroxydisulfate. Chemical Engineering Journal, 2020, 394, 123936.	12.7	63
18	A low-cost photoelectrochemical tandem cell for highly-stable and efficient solar water splitting. Nano Energy, 2017, 41, 225-232.	16.0	62

QINGYI ZENG

#	Article	IF	CITATIONS
19	Polyvinylidene fluoride membrane functionalized with zero valent iron for highly efficient degradation of organic contaminants. Separation and Purification Technology, 2020, 250, 117266.	7.9	60
20	Combined nanostructured Bi2S3/TNA photoanode and Pt/SiPVC photocathode for efficient self-biasing photoelectrochemical hydrogen and electricity generation. Nano Energy, 2014, 9, 152-160.	16.0	59
21	Uranium re-adsorption on uranium mill tailings and environmental implications. Journal of Hazardous Materials, 2021, 416, 126153.	12.4	51
22	Efficient Fenton-like process for organic pollutant degradation on Cu-doped mesoporous polyimide nanocomposites. Environmental Science: Nano, 2019, 6, 798-808.	4.3	49
23	Hierarchically Active Poly(vinylidene fluoride) Membrane Fabricated by In Situ Generated Zero-Valent Iron for Fouling Reduction. ACS Applied Materials & Interfaces, 2020, 12, 10993-11004.	8.0	49
24	A novel 3D ZnO/Cu ₂ O nanowire photocathode material with highly efficient photoelectrocatalytic performance. Journal of Materials Chemistry A, 2015, 3, 22996-23002.	10.3	46
25	Serial hole transfer layers for a BiVO ₄ photoanode with enhanced photoelectrochemical water splitting. Nanoscale, 2018, 10, 18378-18386.	5.6	44
26	Reformed bamboo and reformed bamboo/aluminium composite. Journal of Materials Science, 1994, 29, 5990-5996.	3.7	41
27	Potocatalytic antifouling membrane with dense nano-TiO2 coating for efficient oil-in-water emulsion separation and self-cleaning. Journal of Membrane Science, 2022, 645, 120204.	8.2	41
28	Efficient solar hydrogen production coupled with organics degradation by a hybrid tandem photocatalytic fuel cell using a silicon-doped TiO2 nanorod array with enhanced electronic properties. Journal of Hazardous Materials, 2020, 394, 121425.	12.4	38
29	A self-sustaining monolithic photoelectrocatalytic/photovoltaic system based on a WO3/BiVO4 photoanode and Si PVC for efficiently producing clean energy from refractory organics degradation. Applied Catalysis B: Environmental, 2018, 238, 309-317.	20.2	37
30	Tuning three-dimensional TiO2 nanotube electrode to achieve high utilization of Ti substrate for lithium storage. Electrochimica Acta, 2014, 133, 570-577.	5.2	36
31	Efficient wastewater treatment and simultaneously electricity production using a photocatalytic fuel cell based on the radical chain reactions initiated by dual photoelectrodes. Journal of Hazardous Materials, 2017, 337, 47-54.	12.4	36
32	Self-Driven Photoelectrochemical Splitting of H ₂ S for S and H ₂ Recovery and Simultaneous Electricity Generation. Environmental Science & Technology, 2017, 51, 12965-12971.	10.0	35
33	Exfoliated and plicated g-C3N4 nanosheets for efficient photocatalytic organic degradation and hydrogen evolution. International Journal of Hydrogen Energy, 2021, 46, 20547-20559.	7.1	34
34	The effect and mechanism of organic pollutants oxidation and chemical energy conversion for neutral wastewater via strengthening reactive oxygen species. Science of the Total Environment, 2019, 651, 1226-1235.	8.0	32
35	Idazoxan reduces blood–brain barrier damage during experimental autoimmune encephalomyelitis in mouse. European Journal of Pharmacology, 2014, 736, 70-76.	3.5	30
36	Evaluation of load shedding to prevent dynamic voltage instability based on extended fuzzy reasoning. IET Generation, Transmission and Distribution, 1997, 144, 81.	1.1	29

Qingyi Zeng

#	Article	IF	CITATIONS
37	Efficient electricity production coupled with water treatment via a highly adaptable, successive water-energy synergistic system. Nano Energy, 2020, 67, 104237.	16.0	29
38	Preparation of a BiVO ₄ nanoporous photoanode based on peroxovanadate reduction and conversion for efficient photoelectrochemical performance. Nanoscale, 2018, 10, 2848-2855.	5.6	28
39	Comparative Long-Term Effectiveness of a Monotherapy with Five Antiepileptic Drugs for Focal Epilepsy in Adult Patients: A Prospective Cohort Study. PLoS ONE, 2015, 10, e0131566.	2.5	28
40	Coordination of TCSC and SVC for stability improvement of power systems. , 1997, , .		27
41	Effect of CoOOH loading on the photoelectrocatalytic performance of WO3 nanorod array film. Applied Surface Science, 2013, 284, 285-290.	6.1	27
42	Highly improved photoelectrocatalytic efficiency and stability of WO ₃ photoanodes by the facile <i>in situ</i> growth of TiO ₂ branch overlayers. Nanoscale, 2018, 10, 13393-13401.	5.6	27
43	An ANN-based multilevel classification approach using decomposed input space for transient stability assessment. Electric Power Systems Research, 1998, 46, 259-266.	3.6	26
44	Highly efficient removing refractory organics continuously using a Fenton-like Filter: The role of in-situ galvanic effect enhanced peroxymonosulfate activation. Chemical Engineering Journal, 2022, 450, 138067.	12.7	26
45	Transverse Vibration of Train-Bridge and Train-Track Time Varying System and the Theory of Random Energy Analysis for Train Derailment. Vehicle System Dynamics, 2004, 41, 129-155.	3.7	23
46	Interactive Buckling Behavior and Ultimate Load of I-Section Steel Columns. Journal of Structural Engineering, 1997, 123, 1210-1217.	3.4	22
47	Electronic structures and optical properties of P and Cl atoms adsorbed/substitutionally doped monolayer MoS 2. Solid State Communications, 2018, 280, 6-12.	1.9	22
48	Preparation of hematite with an ultrathin iron titanate layer via an in situ reaction and its stable, long-lived, and excellent photoelectrochemical performance. Applied Catalysis B: Environmental, 2017, 218, 690-699.	20.2	21
49	Highly Efficient Hydrogen and Electricity Production Combined with Degradation of Organics Based on a Novel Solar Water-Energy Nexus System. ACS Applied Materials & Interfaces, 2020, 12, 2505-2515.	8.0	20
50	Investigation of microstructural abnormalities in white and gray matter around hippocampus with diffusion tensor imaging (DTI) in temporal lobe epilepsy (TLE). Epilepsy and Behavior, 2018, 83, 44-49.	1.7	18
51	Reinforcing hydration layer on membrane surface via nano-capturing and hydrothermal crosslinking for fouling reduction. Journal of Membrane Science, 2022, 644, 120076.	8.2	18
52	Risk of seizure relapse after antiepileptic drug withdrawal in adult patients with focal epilepsy. Epilepsy and Behavior, 2016, 64, 233-238.	1.7	16
53	Efficient Degradation of Refractory Organics Using Sulfate Radicals Generated Directly from WO3 Photoelectrode and the Catalytic Reaction of Sulfate. Catalysts, 2017, 7, 346.	3.5	16
54	Preparation of titanium dioxide nanotube arrays on titanium mesh by anodization in (NH ₄) ₂ SO ₄ /NH ₄ F electrolyte. Materials and Corrosion - Werkstoffe Und Korrosion, 2013, 64, 1001-1006.	1.5	15

QINGYI ZENG

#	Article	IF	CITATIONS
55	Dependence of dark current on carrier lifetime for InGaAs/InP avalanche photodiodes. Optical and Quantum Electronics, 2015, 47, 1671-1677.	3.3	15
56	Deriving a transient stability index by neural networks for power-system security assessment. Engineering Applications of Artificial Intelligence, 1998, 11, 771-779.	8.1	14
57	Reformed bamboo/glass fabric/aluminium composite as an ecomaterial. Journal of Materials Science, 1998, 33, 2147-2152.	3.7	12
58	Fuzzy-set approach to dynamic voltage security assessment. IET Generation, Transmission and Distribution, 1995, 142, 190.	1.1	11
59	Improving the charge properties of the WO ₃ photoanode using a BiFeO ₃ ferroelectric nanolayer. Physical Chemistry Chemical Physics, 2021, 23, 8241-8245.	2.8	11
60	FeVO ₄ Nanopolyhedron Photoelectrodes for Stable and Efficient Water Splitting. ChemSusChem, 2021, 14, 3010-3017.	6.8	11
61	Relative Seizure Relapse Risks Associated with Antiepileptic Drug Withdrawal After Different Seizure-Free Periods in Adults with Focal Epilepsy: A Prospective, Controlled Follow-Up Study. CNS Drugs, 2019, 33, 1121-1132.	5.9	10
62	Substitution has better efficacy than add-on therapy for patients with focal epilepsy after their first antiepileptic drug treatments fail. Seizure: the Journal of the British Epilepsy Association, 2019, 64, 23-28.	2.0	9
63	Numerical analysis of multiplication layer on dark current for InGaAs/InP single photon avalanche diodes. Optical and Quantum Electronics, 2014, 46, 1203-1208.	3.3	7
64	Branched core-shell a-TiO2@N-TiO2 nanospheres with gradient-doped N for highly efficient photocatalytic applications. Chinese Chemical Letters, 2023, 34, 107628.	9.0	7
65	Investigation of the Impact Toughness of Normal Bamboo, Reformed Bamboo and Reformed Bamboo Composites. Science and Engineering of Composite Materials, 1995, 4, 255-260.	1.4	6
66	High repetition rate pulsed laser of twin wavelengths from KTiOPO 4 optical parametric oscillation. Chinese Physics B, 2004, 13, 1402-1406.	1.3	6
67	Fabrication of TiO2/CdS/TiO2 Nanotube/Ti Mesh Electrode and Application in Photoelectro-catalytic Cell System for Degradation of Methylene Blue under Visible Light Illumination. Asian Journal of Chemistry, 2013, 25, 8527-8532.	0.3	6
68	Fuzzy reasoning for knowledge-based assessment of dynamic voltage security. IET Generation, Transmission and Distribution, 1996, 143, 157.	1.1	5
69	Reformed bamboo and reformed bamboo/aluminium composite Part II impact properties. Journal of Materials Science Letters, 1996, 15, 129-131.	0.5	5
70	Residual properties of reformed bamboo/aluminium laminates after hygrothermal aging. Composites Science and Technology, 2001, 61, 1041-1048.	7.8	5
71	Investigation of extended fuzzy reasoning and neural classification for load-shedding prediction to prevent voltage instability. Electric Power Systems Research, 1997, 43, 81-87.	3.6	4
72	A HIGH-ORDER FINITE ELEMENT FORMULATION FOR VIBRATION ANALYSIS OF BEAM-TYPE STRUCTURES. International Journal of Structural Stability and Dynamics, 2009, 09, 649-660.	2.4	4

QINGYI ZENG

#	Article	IF	CITATIONS
73	A novel approach to elasto-plastic finite element analysis of beam structures using the concept of incremental secant stiffness. Finite Elements in Analysis and Design, 2010, 46, 982-991.	3.2	4
74	The transport properties of the Phosphorus and Chlorine doped single layer MoS 2 p–n junctions: A first-principles study. Solid State Communications, 2016, 246, 82-87.	1.9	4
75	Input space decomposition and multilevel classification approach for ANN-based transient security assessment. , 1997, , .		3
76	On generalized extending modules. Journal of Zhejiang University: Science A, 2007, 8, 939-945.	2.4	3
77	Ordered Ti-doped FeVO4 nanoblock photoanode with improved charge properties for efficient solar water splitting. Journal of Colloid and Interface Science, 2021, 604, 562-567.	9.4	3
78	Fuzzy assessment of power system transient stability level based on steady-state data. IET Generation, Transmission and Distribution, 1997, 144, 525.	1.1	2
79	Brewster-oriented passive Q-switch intracavity optical parametric oscillator. Chinese Physics B, 2005, 14, 714-719.	1.3	2
80	Line by line correction of teletext data under multipath transmission. IEEE Transactions on Consumer Electronics, 1992, 38, 874-877.	3.6	1
81	A hybrid framework of short-duration simulation and ANN-based transient stability assessment for contingency screening. , 0, , .		1
82	On generalized CS-modules. Czechoslovak Mathematical Journal, 2015, 65, 891-904.	0.3	1
83	The equation of state of nuclear matter with consideration of clusters and the Pauli-blocking effect. Journal of Physics G: Nuclear Physics, 1988, 14, 1283-1300.	0.8	0
84	Experimental investigation of biomimetic double-helical reinforcing elements. Journal of Materials Science Letters, 1995, 14, 769-772.	0.5	0
85	Dynamic voltage security assessment using a fuzzy severity index. Engineering Applications of Artificial Intelligence, 1995, 8, 657-664.	8.1	0
86	Three-dimensional analysis on plates. Applied Mathematics and Mechanics (English Edition), 1997, 18, 891-903.	3.6	0
87	An automatic method of area change detection based on histogram matching and morphological operation in high spatial remote sensed imagery. , 0, , .		0
88	Angle tuned mid-infrared optical parametric oscillator based on Nd:YAG pumped MgO:LiNbO 3. , 2006, , .		0